ChemPubSoc Europe

DOI: 10.1002/slct.201800412

Chemistry SELECT Full Papers

Check for updates

Electro, Physical & Theoretical Chemistry

Investigation of Structural, Vibrational Properties and Electronic Structure of Fluorene-9-Bisphenol: A DFT Approach

Selin Özkan Kotiloğlu,[a] Sibel Çelik,[b] Emine Tanış,[c] and Mustafa Kurban*[d]

Bisphenol A (BPA) is a chemical used in a variety of materials and has adverse effects on endocrine system. The substitutes of BPA have been developed to produce BPA-free plastics. Fluorene-9-bisphenol (BPFL), has anti-oestrogenic effects, is one of those substitutes used in 'BPA-free' bottles. In this study, the physical, electronic and vibrational properties of BPFL molecule are investigated using density functional theory (DFT) calculations at B3LYP/6-311G (d, p) basis set. Bond distances, Fourier transform **infrared** (FT-IR) spectra, natural atomic charges, solvation energies, dipole moments and vibrational frequencies were carried out. The calculated bond distance for the optimized geometry of BPFL obtained from DFT calculations were compared with the measured results. Structural properties like radial distribution function (RDF) and probability distribution depending on coordination number have been calculated for the molecule. Ultraviolet–visible (UV-Vis) spectra characteristics and the electronic features, such as absorption wavelengths, frontier orbitals, excitation energies and band gap energy of BPFL were also recorded using time-dependent (TD) DFT approach based on optimized structure with different solvent environments. Finally, we investigated the effects of solvents on structural, electronic and vibrational frequencies of BPFL molecule.

1. Introduction

Endocrine disrupting-chemicals (EDCs) are synthetic chemicals that can mimic or block endocrine functions.[1] They may alter various hormonal processes resulting perturbed reproductive, metabolic and developmental effects and therefore they are defined as a health threat to human and wild life population.[2,3] Insecticides, herbicides, fungicides, organochlorides, synthetic hormones, some pharmaceutical drugs, various industrial chemicals, plasticizers such as phthalates and bisphenols are the common groups with endocrine activity.[4,5]

Bisphenols are widely used plasticizers providing flexibility to polycarbonate and epoxy resin plastics and known as endocrine disrupting chemicals due to their binding ability to human nuclear receptors.[5] This group of chemicals consist of two phenol rings and a linker atom that is usually carbon.[6] Its phenyl group mimics estrogen which resulting in estrogen receptor binding.[5,7] Every people are being exposed to those chemicals as they are frequently in use since the industrial revolution.[6,8] Bisphenol A (BPA) is a well-studied EDC and classified as reproductive toxicant amongst bisphenols. It was synthesized in 1905, has been used in the manufacturing of polycarbonate (used for water bottles), epoxy resins (used for construction materials and canned food) and thermal paper.[9,10] Its estrogenic activity was reported firstly in 1936.[11] Due to the continuous exposure, BPA can be detected in human tissue and body fluids such as placental tissue, serum, breast milk, urine.[12–14] It is commonly used in toys, dental products, plastic baby bottles, and food and beverage packages and thus has direct contact with consumed foods and believed to be leached from them.[12] Therefore, its usage in children products is being limited in recent years, which has led to the development of the alternatives of BPA. BPA alternatives, which are mostly analogous of BPA such as Bisphenol S (BPS), Bisphenol F (BPF), are frequently preferred in the production "BPA-free" materials since they are considered safer than BPA.[14] BPS and BPF are used for many industrial applications such as production of cleaning products, thermal paper, industrial floors, adhesives, water pipes, dental sealents, and food packages. It have also been detected in food, personal care and paper products.[15] However, the effects of BPA alternatives on health are still unclear and those alternatives are being suspected to have similar toxic effects.[16]

Fluorene-9-bisphenol (BPFL) is a kind of bisphenol fluorene with cardo skeleton. It is mostly exploited for the production of polyarylates, polyesters, polyethers, polycarbonates, polyurethanes and epoxy resins since its cardo rings provide unique characteristics. Due to these cardo polymer features such as high transparency, thermal stability, insulation and high-

[a] *Dr. S. Ö. Kotiloğlu*
Department of Molecular Biology and Genetics, Ahi Evran University, 40100 Kırşehir, Turkey
[b] *Dr. S. Çelik*
Vocational School of Health Services, Ahi Evran University, 40100 Kırşehir, Turkey
[c] *Dr. E. Tanış*
Kaman Vocational School, Ahi Evran University, 40100 Kırşehir, Turkey
[d] *Dr. M. Kurban*
Department of Electronics and Automation, Ahi Evran University, 40100 Kırşehir, Turkey
E-Mail address:
E-mail: mkurbanphys@gmail.com

Supporting information for this article is available on the WWW under https://doi.org/10.1002/slct.201800412

© 2018 Wiley-VCH Verlag GmbH & Co. KGaA, Weinheim

refractive index, BPFL has been preferred in industrial applications.[17,18] The structure of Fluorene-9-bisphenol, which consists of a cardo unit connected with two phenolic groups, is akin to the structure of BPA (see Figure 1). Hence, BPFL is used as a

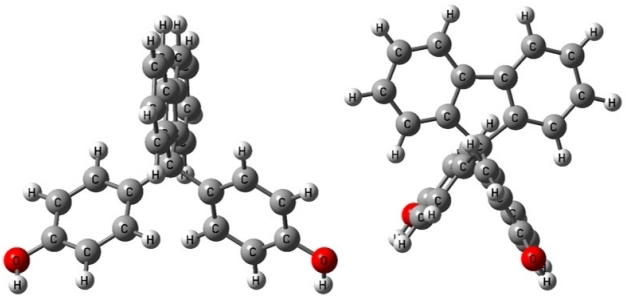

Figure 1. (Colour online) Different views of optimized ground state geometry of BPFL molecule with atom numbering calculated by B3LYP/6-311G (d, p).

substitute of BPA in the production of "BPA-free" plastics.[19] The estrogenic activity of BPA and its substitutes are known to cause various reproductive and metabolic disorders such as obesity, type-2 diabetes mellitus.[20,21] However human exposure to BPFL and its effects is not yet clear. Recently, Fluorene-9-bisphenol, which has been preferred frequently in production of moulded matrices, epoxy floor coatings, insulation materials, and milk and baby bottles, has been found to be released from them and can be detected in serum of exposed female mice. Additionally, those mice were determined to have low uterine weights and less estrogen-related gene expressions. Thus, it was shown that BPFL has strong anti-estrogenic activity.[19]

The solute-solvent interactions are crucial to understand molecular behaviour as solvent effect may lead significant changes.[22] With the help of the new methodologies allowing the detection of solvent effect, solute-solvent interactions were found to be responsible for the significant changes in the chemical and physical characteristics of the solute in going from gas phase to solvent phase. Therefore investigating the effect of the solvent is critical to understand the various properties of molecules of interest.[22] Correspondingly, the importance of studying the effects of solvation relies on the differences of the structure and reactivity of free molecules from that in the solvent environment. Furthermore, solvent effects are pivotal tools to design new drugs since the properties of a drug such as absorption, release and transport in the body are affected by them and are meaningful for the future drug design attempts. The necessity of detailed examination of the interactions between the solute and the solvent molecules makes it a difficult task.[23] Furthermore, the probability of theoretical estimation of solvent effects on the characteristics of molecules is still a challenge in computational chemistry as the most of the important chemical and biological reactions occur in solution.[24]

To our knowledge, there have not been any reports about the structural, electronic, spectroscopic and optical properties of BPFL molecule using quantum chemical calculations. In this regard, we aim to investigate the physical, electronic and vibrational features of BPFL molecule using density functional theory (DFT) calculations at B3LYP/6-311G (d, p) basis set. Finally, we investigated the effects of solvents on structural, electronic and vibrational frequencies of BPFL molecule.

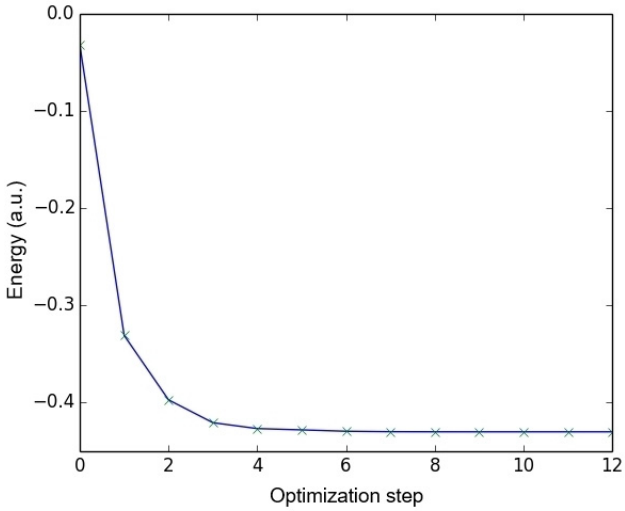

Figure 2. (Colour online) Process of geometry optimization of BPFL molecule.

2. Computational details

The geometrical, energetic, electronic and spectroscopic properties of BPFL were investigated using DFT[25] at the B3LYP level.[26–28] The 6–311G (d, p) basis set was used in the calculations. In order to test the validity and reliability of our calculations, CAM–B3LYP[29] functional were also tested for accuracy and efficiency of the calculations because B3LYP actually underestimates HOMO-LUMO gaps and underestimate excited-state energies.[30–32] The calculations were performed using the GAUSSIAN09 program package.[33] Various spin multiplicities were investigated and it was found that BPFL has spin singlet in terms of the most stable structure with minimum total energy. The structure was taken as the local minima on potential energy surface having positive vibration frequencies. After geometric optimization, TD-DFT method was utilized to get maximum wavelengths, the highest occupied molecular orbital (HOMO), the lowest unoccupied molecular orbital (LUMO) and the frontier molecular orbital energy gap (HOMO–LUMO difference in energy gap, E_g) of BPFL. Optimized ground state structure and process of geometry optimization of BPFL with atom numbering calculated by B3LYP/6-311G (d, p) are shown in Figs. 1 and 2, respectively.

© 2018 Wiley-VCH Verlag GmbH & Co. KGaA, Weinheim

3. Results and discussion

3.1 Structural analysis

Playing a critical role in understanding different physical and biological properties of molecules, the interactions between the solute and solvent molecules are needed to be profoundly examined since the structure of free molecules are very different from that in the solvent environment. This section elaborates on the solvent effects on the geometrical parameters.

Initially, the reoptimized calculation was performed in different solutions using the gas phase as starting points with B3LYP/6-311G (d, p) and B3LYP/6-311++G (d, p) employing the PCM model within SCRF theory. The selected bond lengths of BPFL structure in gas phase and solvents are listed in Table 1.

Table 1. Solvation energies ($\Delta E_s = E_{solution}$ - E_{gas}, in kJ/mol), solvation free energies ($\Delta G_s = G_{solv}$ - G_{gas}, in kJ/mol), and dipol moments μ (in Debye) of BPFL in the gas phase and in different solvents.

	Gas ($\varepsilon = 1$)	Ethanol ($\varepsilon = 24.5$)	Acetonitrile ($\varepsilon = 36.6$)	Water ($\varepsilon = 80.1$)
ΔE_s	0.0	-38.59	-39.38	-40.69
ΔG_s	0.0	- 42.49	- 43.31	- 44.26
μ	1.90	2.62	2.64	2.68

On the whole, the geometrical structures were influenced by the solvent effects. As observed in the solid phase these results showed geometric changes due to solvation. Even though crystal phase are required to make a correct description, the theoretical calculations provide qualitative observation into the solvent effects on equilibrium structures of the molecule.

Computed geometrical parameters in the gas phase were rather consistent with the experimental X-ray diffraction results.[34] (see Table S1 in the Supporting Information). Deviation from the experimental data was within 0.0515 Å at B3LYP/6-311G (d, p) level, and 0.0517 Å at B3LYP/6-311++G (d, p) level. The optimized parameters obtained by applying the B3LYP/6-311G (d, p) and B3LYP/3-311++G (d, p) levels were almost similar. These results indicated that the values calculated by B3LYP/6-311G (d, p) basis set were more concordant with the experimental values with respect to those calculated by B3LYP/6-311++G (d, p) method. Hence, only the results from the B3LYP/6-311G (d, p) calculations were further discussed.

Table S2 in the Supporting Information presents the changes in theoretical geometrical parameters of BPFL while passing from the gas phase to solution. As a result of solvent effects, calculated geometrical parameters of BPFL in various media revealed some small but significant deviations.

The computed geometrical parameters of BPFL were observed as changing gradually with the increasing dielectric constant (ε) of medium. Changes in geometrical parameters, though they were slight, were found to be significant while passing from the gas phase to solution. For example, the O–H, C–O and C–C bond lengths changed slightly with the solvent polarity (Table S2 in the Supporting Information). The calculated values at the B3LYP/6-311G (d, p) level were obtained as follows: O–H bond length 0.962 Å, C–O bond length 1.366 Å for the gas phase. The experimental bond distance 0.840 Å, and 1.367 Å revealed a good agreement with the results of X-ray diffraction experiment.

Analysis of calculation results showed that, ongoing from gas phase to solutions, there was a slight change in the bond lengths. For example, several bond lengths like C–C, C–H and O–H were predicted to be shorter in the gas phase comparing to those in the solvents, whereas C–O bonds were calculated longer in the gas phase than those in solvent media.

The changes in the geometrical parameters of molecule were regarded as a result of the electrostatic interactions between the solute and the solvent.

3.2. Charge Distribution

The atomic charges in BPFL molecule in the gas and solvation phases computed by natural population analysis (NPA) with B3LYP/6-311G (d, p) level are demonstrated in Table S3 in the Supporting Information. This calculation detailed the charges of the every atom in the molecule. Distribution of positive and negative charges is crucial to understand the increase or decrease of the bond length between the atoms. Generally, the presence of solvent surrounding may modify the electron distribution of a molecule in gas phase. Thus, understanding the chemistry of molecules in solutions is critical.[35]

The solvent effect caused drastic changes in the atomic net charges for several atoms. Results in Table S3 in the Supporting Information show that all oxygen atoms and carbon atoms are negatively charged, C–O bond carbon atoms are positively charged. The negative charges on carbon and oxygen atoms increased with the increasing solvent polarity. The positive charges on carbon atoms and hydrogen atoms increased with the increase in dielectric constants of solvents.

These can be interpreted by the fact that the oxygen atom is more negative than carbon and hydrogen atoms, and has lone pair of electrons by which it easily interacts with the solvents.

For instance, the largest negative charge (−0.670 e) was localized on oxygen atom with increasing polarity, while the positive charges on C26, C27, 4C and 5C atoms. It is also observed slight drop in the charges of 4C (from 0.042 e to 0.037 e) and C26 and C27 atoms (from 0.333 e to 0.328 e). Hence, we have concluded that the negative charge led to the redistribution of electron density. On the other hand, the positive charges increase from gas phase to solvation phase. The calculated distribution of positive charges on all hydrogen atoms were regularly increasing with the increasing dielectric constant (ε) of the medium. The maximum atomic charge was observed on O atom comparing to other atoms in solvent environments. Thus one can conclude that the charge distributions are sensitive to dielectric medium.

© 2018 Wiley-VCH Verlag GmbH & Co. KGaA, Weinheim

3.3. Solvation energy, solvation free energy, and dipole moment

Table 1 includes the calculation results for solvation energies ΔE_{solv}, solvation free energies ΔG_{solv}, and dipole moments of BPFL in the gas phase, and in different solvents predicted at B3LYP/6-311G (d, p) level of theory.

The dipole moment is expected to be larger in solution than the corresponding dipole moment in the gas phase. The dipole moments increased from gas phase to solvation phase, mainly due to major charge redistribution in the molecule, and also by charges in the distances between the charge separations.[36] The dipole moment of BPFL molecule was found out as 1.90 Debye in the gas phase and 2.62, 2.64 and 2.68 Debye in ethanol, acetonitrile (ACN), and water, respectively.

The energy of solvation is related with the dipole moment. The large dipole moment means the stronger solvation energy,[36] thus it leads to larger stabilization in solution phase. In addition, the solvation energies are usually not dependent on strongly basis set or model.[37] The solvent with larger dielectric constant gave rise to larger stabilization energy for polar species. Relatively, the stabilizing effect of water ($\varepsilon = 80.1$) was greater than the ACN ($\varepsilon = 36.6$). The stabilization energies increased on going from the gas phase to solution phase, and the best solvation state was also the water due to its charge and higher dipole moment value as given in Table 1. The relative energies decreased while the solvation energies and dipole moments increased with increment of dielectric constant of solvent (Table 1).

The solvation free energy, ΔG_{solv}, which is the work needed to transfer molecule from gas phase into solution, plays a significant role in the understanding of the chemical and biological behaviour of molecules in condensed phase.[38] Calculated ΔG_{solv} of BPFL are listed in Table 1. It can be observed that the ΔG_{solv} value increased with the increase of the solvent polarity, and thus, the solvation of BPFL increased with the polarity of the solvent. The value of ΔG_{water} was more negative than that of ethanol and ACN that means that the solvation of BPFL in water was better than in other solvent. In addition, the data of ΔG_{solv} value showed that the solvation of the title molecule increased with the growing of the solvent polarity. The solvation free energies could be explained by the difference in polarity. The computed ordering of the solvation free energies in several solvents was as follows: water > ethanol > ACN. That is to say, BPFL molecule was more soluble in water than in the less ethanol or ACN solvents. Our theoretical results revealed that solubility of BPFL decreased in the order of water > ethanol > ACN using PCM method.

Since it represents the desolvation cost of a ligand binding to a receptor, solvation free energy is considered as an important molecular characteristic in drug discovery studies. Most of the recent developments in the estimation of solvation free energy require the use of molecular mechanics and dynamics calculations.

3.4. Vibrational Frequencies and Infrared Spectra

Vibrational spectroscopy is very sensitive method to probe the solute-solvent interactions. Solvent interaction has a major role in the crucial biological reactions occurring in solution phase.[39]

This section presents and discusses the results, including solvent effect on the vibrational frequencies and Fourier transform infrared (FT-IR) spectra of BPFL in different phase. Experimental (solid state) and theoretical FT-IR (in gas phase and various solvents) spectra were plotted against the harmonic vibrational frequencies of BPFL (see Figure 3). From Figure 3,

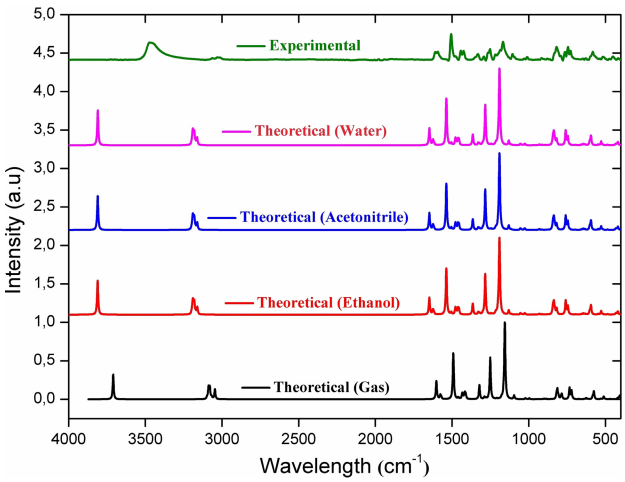

Figure 3. (Colour online) Experimental (solid state) and theoretical (in gas phase and various solvents) FT-IR spectra of BPFL molecule for different solvents.

we note that the presence of a dielectric medium is not strong influence on the calculated vibrational frequencies. The changes in the calculated frequencies scaled by 0.9682[40] on going from the gas phase to media are tabulated in Table S4 in the Supporting Information. All optimizations were carried out at B3LYP/6-311G (d, p) level. Gas phase geometry was used as starting structure in the further calculations.

Apparently, the frequencies of all bands were shifted from gas phase to solution though most of the shifts were observed as relatively small. The calculated IR intensities also changed regularly with the increasing solvent polarity. In solution, the modes 1, 64, 65, 112, 113, 128, 129 shifted to higher values while the other vibrational modes shifted to lower values. The C=C stretching vibration computed at 1603 cm^{-1} (scaled value) showed excellent agreement with FT-IR 1608 cm^{-1} (strong) bands. The bands at 1505 (very strong) and 1593 cm^{-1} (strong) in FT-IR spectrum were assigned to C–O stretching. The bands observed at 3029 (weak) and 3018 cm^{-1} (weak) in FT-IR were assigned to C–H stretching vibrations of the phenyl rings. The υ(OH) stretching vibration is generally observed in the region around 3600 cm^{-1}.[41] The band observed at 3471 cm^{-1} (shoulder) was assigned to O–H stretching vibration. The theoretically computed values at 813, 1096, 1155, 1209, 1251 cm^{-1} were

© 2018 Wiley-VCH Verlag GmbH & Co. KGaA, Weinheim

Table 2. The Computed absorption wavelength (λ, in nm), excitation energies (E, in eV), absorbance and oscillator strengths of BPFL for gas phase and different solvents.

Gas			Ethanol			Acetonitrile			Water		
λ	*E*	*f*	λ	*E*	*f*	λ	*E*	*f*	λ	*E*	*f*
300.97	4.11	0.03	301.34	4.11	0.04	301.35	4.11	0.04	301.38	4.11	0.04
291.94	4.24	0.04	293.37	4.22	0.06	293.38	4.22	0.06	293.40	4.22	0.06
280.46	4.42	0.01	279.96	4.42	0.01	79.94	4.42	0.01	279.92	4.42	0.01

found to be good agreement with the experimental data by B3LYP/6-311G (d, p) method (mode nos. 50, 74, 79, 85 and 86) (see Table S4 in the Supporting Information).

3.5. Electronic properties

The absorption wavelength, excitation energies, absorbance and oscillator strengths of BPFL molecule for different solvents at B3LYP/6-311G (d, p) level of theory (in the wavelength range 230–320 cm^{-1}) are listed in Table 2. Figure 4 shows absorption

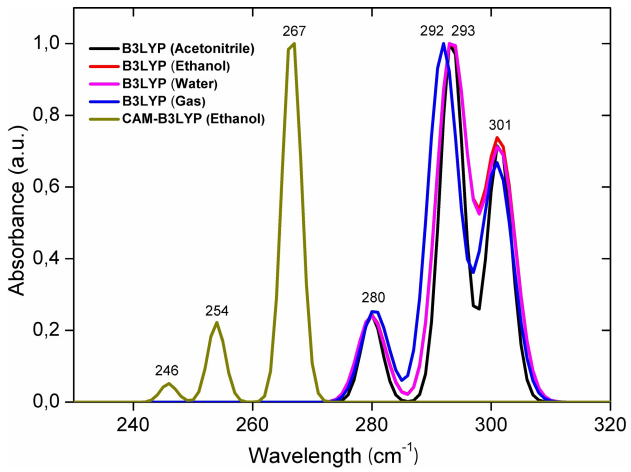

Figure 4. (Colour online) UV absorbance plots vs. wavelength of BPFL molecule for different solvents and functionals.

spectra of BPFL molecule ACN, ethanol, water and gas phase. Absorption wavelengths were found to be nearly the same for all solvent which calculated as 280, 292, 293 and 301 cm^{-1} so the molecule may not be affected the solvents. The energy value for CAM–B3LYP functional (267 cm^{-1}) are found to be significantly different than that of B3LYP functional (301 cm^{-1}). We also plotted the absorption wavelength obtained from CAM–B3LYP functional for ethanol in Figure 4.

3.6. Frontier molecular orbitals analysis

In a molecule, the highest occupied molecular orbital (HOMO) and the lowest unoccupied molecular orbital (LUMO) are called as frontier molecular orbitals (FMOs). While the HOMO energy is related to the ionization potential, the LUMO energy is related to the electron affinity.[42,43] This is also employed by the frontier electron density to estimate the most reactive position in π-electron systems and also explains various types of reaction in conjugated system.[44] A small highest occupied molecular orbital–lowest unoccupied molecular orbital (H–L) separation, which is the outcome of an important degree of intra-molecular charge transfer from the end-capping electron donor groups to the efficient electron-acceptor group through-π conjugated path, is used to characterize the conjugated molecules.[45] The energy gap between HOMO and LUMO is an indicator of bioactivity as it shows the correlation between biological systems and chemicals. The smaller value implies the low stability for the molecule meaning higher reactivity in chemical reactions.[46,47]

The density of states (DOS or TDOS) is essentially the number of different states at a particular energy level. DOS is important, because the occupied and unoccupied molecular orbitals can be seen on DOS spectrum. Using Mulliken population analysis, we have plotted total density of state (TDOS) spectrum (see Figure 5). The FMOs energy was calcu-

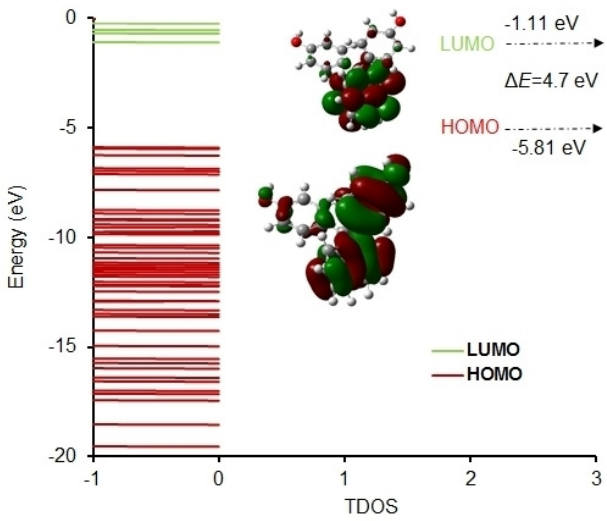

Figure 5. (Colour online) The molecular orbitals and energy gap (ΔE) between frontier HOMO and LUMO of BPFL molecule. Green and red colours represent the positive and negative isosurfaces for HUMO and LUMO, respectively.

lated by B3LYP/6-311++G (d, p) method for ACN, ethanol, water solutions and gas phase: $E_{HOMO} = -5.81$ eV, $E_{LUMO} = -1.11$ eV $E_{HOMO-LUMO} = 4.71$ eV for B3LYP functional. The

© 2018 Wiley-VCH Verlag GmbH & Co. KGaA, Weinheim

calculated HOMO, LUMO and HOMO-LUMO energy gap with CAM–B3LYP are found 7.48, 0.26 and 4.86 eV, respectively. The energy gap which is energy difference between HOMO and LUMO orbital is a crucial parameter in measuring the electron conductivity. This value was calculated in four solvents and presented in Table 3.

Table 3. The calculated HOMO (E_{HOMO}), LUMO (E_{LUMO}) energies and energy gaps (E_g) (in eV) between HOMO and LUMO, chemical hardness (η), electronegativity (χ), chemical potential (μ) and electrophilicity index (ω) of BPFL for gas phase and different solvents.

Solvent	E_{HOMO}	E_{LUMO}	E_g	η	χ	μ	ω
Acetonitrile	-5.98	-1.27	4.71	2.36	3.63	-3.63	2.79
Gas	-5.81	-1.11	4.70	2.35	3.46	-3.46	2.54
Ethanol	-5.98	-1.27	4.71	2.36	3.62	-3.62	2.78
Water	-5.99	-1.28	4.71	2.36	3.63	-3.63	2.80

The value of chemical hardness (η) was 2.36 eV in ACN, ethanol and water solvents, it was decreasing 0.01 eV in gas phase. Electronegativity and chemical potential were the same, but the value of electrophilicity index was different in all solvents.

3.7. Radial Distribution Function and Probability Density

To investigate the difference between carbon-carbon (C–C), carbon-oxygen (C–O), carbon-hydrogen (C–H) and oxygen-hydrogen (O–H), we plotted the radial distribution functions (RDF) of C–C, C–O, C–H and O–H atoms in gas phase in Figure 6. One can see that C–C had a narrower and higher

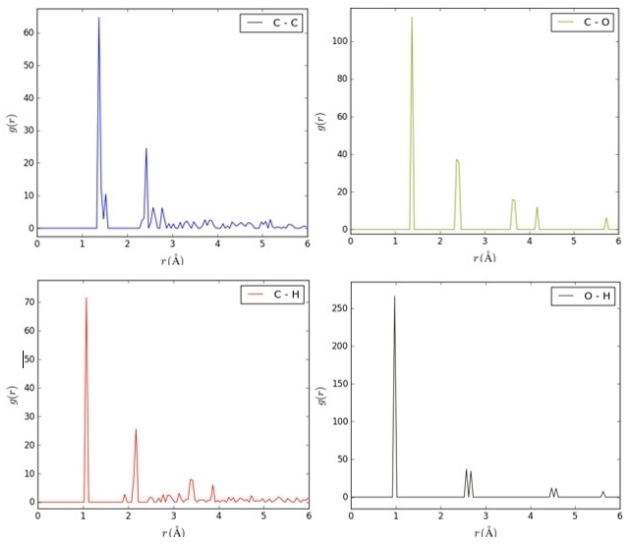

Figure 6. Radial distribution functions (RDFs) for carbon-carbon (C–C), carbon-oxygen (C–O), carbon-hydrogen (C–H) and oxygen-hydrogen (O–H) atoms in gas phase.

distribution. In addition, there was a slight difference between C–C and C–H atoms. For C atoms, C–O was slightly shorter than C–C; for H, O–H was shorter than C–H. Taking into consideration all of the combinations, C–O had stronger interactions than the other ones (especially interactions with H). To study the influence of interactions of the atoms in the molecule, we also performed the probability distribution depending on the coordination number (Figure 7). The coordination number of C–H interactions decreased significantly O–H hydrogen bonding interaction becomes weak due to lower cohesive energy between C–H interactions. The overall C–C coordination number also decreased from 1.60 to 0.12 due to the different dimer effects.

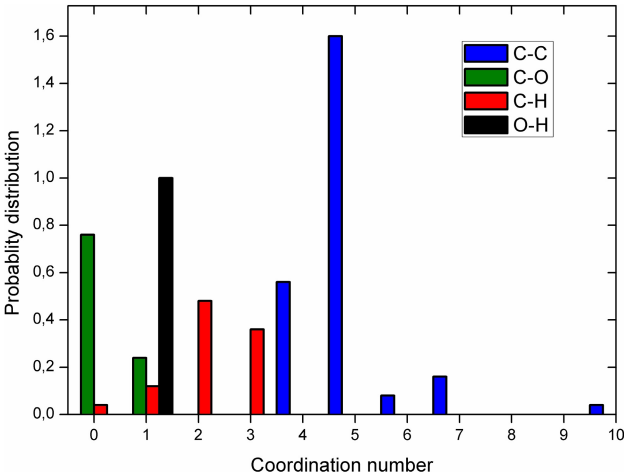

Figure 7. Probability distributions of carbon-carbon (C–C), carbon-oxygen (C–O), carbon-hydrogen (C–H) and oxygen-hydrogen (O–H) atoms in gas phase.

4. Conclusions

In the present work spectroscopic and electronic properties of BPFL molecule for different solvents were investigated using DFT calculations in detail and compared with experimental results in the literature. The calculated geometrical parameters of BPFL molecule were showed small but significant deviations in solvent environment and found to be consistent with experimental results. The vibrational frequencies, solvent energies, dipole moments and charge distributions changed with the increasing solvent polarity whereas the electronic properties were not affected in solvent media. Radial distribution function and probability distribution were also searched. We hope that this study will provide an insight for new studies on physical properties of chemicals with estrogenic activities.

Supplementary data

Supplementary material related to this article can be found, in the online version.

© 2018 Wiley-VCH Verlag GmbH & Co. KGaA, Weinheim

Conflict of Interest

The authors declare no conflict of interest.

Keywords: DFT · Electronic properties · Fluorene-9-bisphenol · HOMO-LUMO · Structure analysis

[1] US Environmental Protection Agency. Memorandum to EDSTAC Members RE: Definition of "Endocrine Disruptor". Washington D. C., USA, **2007**.
[2] R. T. Zoeller, T. R. Brown, L. L. Doan, A. C. Gore, N. E. Skakkebaek, A. M. Soto, T. J. Woodruff, F. S. V. Saal, *Endocrinology* **2012**, *153*, 4097–4110.
[3] M. F. Sweeney, N. Hasan, A. M. Soto, C. Sonnenschein, *Rev. Endocr. Metab. Disord.* **2015**, *16*, 341–357.
[4] S. Flint, T. Markle, S. Thompson, E. Wallace, *J. Environ. Manage.* **2012**, *104*, 19–34.
[5] A. C. Gore, V. A. Chappell, S. E. Fenton, J. A. Flaws, A. Nadal, G. S. Prins, J. Toppari, R. T. Zoeller, *Endocr Rev.* **2015**, *36*, E1–E150.
[6] S. D. Gramec, M. L. Peterlin, *Environ. Toxicol. Pharmacol.* **2016**, *47*, 182–199.
[7] M. G. Zlatnik, *J. Midwifery Wom. Heal.* **2016**, *61*, 442–455.
[8] M. Z. Jeddi, L. Janani, A. H. Memari, S. Akhondzadeh, M. Yunesian, *Environ Res.* **2016**, *151*, 493–504.
[9] J. D. Meeker, *Arch. Pediatr. Adolesc. Med.* **2012**, *166*, E1–7.
[10] J. Michalowicz, *Environ. Toxicol. Pharmacol.* **2014**, *37*, 738–758.
[11] E. C. Dodds, W. Lawson, *Nature* **1996**, *137*, 996.
[12] L. N. Vandenberg, R. Hauser, M. Marcus, N. Olea, W. V. Welshons, *Reprod. Toxicol.* **2007**, *24*, 139–177.
[13] A. M. Calafat, X. Ye, L–Y. Wong, J. A. Reidy, L. L. Needham, *Environ. Health. Perspect.* **2008**, *116*, 39–44.
[14] X. Ye, L. Y. Wong, J. Kramer, X. Zhou, T. Jia, A. M. Calafat, *Environ. Sci. Technol.* **2015**, *49*, 11834–11839.
[15] J. R. Rochester, A. L. Bolden, *Environ. Health. Perspect.* **2015**, *123*, 643–650.
[16] S. Rattan, C. Zhou, C. Chiang, S. Mahalingam, E. Brehm, J. A. Flaws, *J. Endocrinol.* **2017**, *233*, R109–R129.
[17] V. V. Korshak, S. V. Vinogradova, Y. S. Vygodskii, *J. Macromol. Sci. Rev. Macromol. Chem. Phys.* **1974**, *11*, 45–142.
[18] W. Liu, J. Wang, Q. H. Qiu, L. Ji, C. Y. Wang, M. L. Zhang, *Pigm. Resin. Technol.* **2008**, *37*, 9–15.
[19] Z. Zhang, Y. Hu, J. Guo, L. Sun, X. Xiao, D. Zhu, T. Nakanishi, Y. Hiromori, J. Li, X. Fan, Y. Wan, S. Cheng, J. Li, X. Guo, J. Hu, *Nat. Commun.* **2017**, *8*, 14585(1-13).
[20] T. Wang, M. Li, B. Chen, M. Xu, Y. Xu, Y. Huang, J. Lu, Y. Chen, W. Wang, X. Li, Y. Liu, Y. Bi, S. Lai, G. Ninq, *J. Clin. Endocrinol Metab.* **2012**, *97*, E223–227.
[21] M. M. Stojanoska, N. Milosevic, N. Milic, L. Abenavoli, *Endocrine* **2017**, *55*, 666–681.
[22] Y. Liu, H. Du, G. Wang, X. Gong, L. Wang, H. Xiao, *Int. J. Quant. Chem.* **2011**, *111*, 1115–1126.
[23] V. Enchev, N. Markova, S. Angelova, *J. Phys. Chem. A* **2005**, *109*, 8904–8913.
[24] A. M. El-Nahas, K. Hirao, *J. Mol. Struct.-Theochem.* **1999**, *459*, 229–237.
[25] W. Kohn, L. J. Sham, *Phys. Rev.* **1965**, *140*, A1133–A1138.
[26] A. D. Becke, *Phys. Rev. A* **1988**, *38*, 3098–3100.
[27] S. H. Vosko, L. Vilk, M. Nusair, *Can. J. Phys.* **1980**, *58*, 1200–1211.
[28] C. Lee, W. Yang, R. G. Parr, *Phys. Rev. B. Condens. Matter.* **1988**, *37*, 785–789.
[29] T. Yanai, D. P. Tew, N. C. Handy, *Chem. Pys. Lett.* **2004**, *393*, 51–57.
[30] M. E. Foster, B. M. Wong, *J. Chem. Theory. Comput.* **2012**, *8*, 2682–2687.
[31] A. Prlj, B. F. E. Curchod, A. Fabrizio, L. Floryan, C. Corminboeuf, *J. Phys. Chem. Lett.* **2015**, *6*, 13–21.
[32] B. Gündüz, M. Kurban, *Vib. Spectrosc.* **2018**, *96*, 46–51.
[33] M. J. Frisch, G. W. Trucks, H. B. Schlegel, G. E. Scuseria, M. A. Robb, J. R. Cheeseman, G. Scalmani, V. Barone, B. Mennucci, G. A. Petersson, H. Nakatsuji, M. Caricato, X. Li, H. P. Hratchian, A. F. Izmaylov, J. Bloino, G. Zheng, J. L. Sonnenberg, M. Hada, M. Ehara, K. Toyota, R. Fukuda, J. Hasegawa, M. Ishida, T. Nakajima, Y. Honda, O. Kitao, H. Nakai, T. Vreven, J. A. Montgomery, Jr., J. E. Peralta, F. Ogliaro, M. Bearpark, J. J. Heyd, E. Brothers, K. N. Kudin, V. N. Staroverov, R. Kobayashi, J. Normand, K. Raghavachari, A. Rendell, J. C. Burant, S. S. Iyengar, J. Tomasi, M. Cossi, N. Rega, J. M. Millam, M. Klene, J. E. Knox, J. B. Cross, V. Bakken, C. Adamo, J. Jaramillo, R. Gomperts, R. E. Stratmann, O. Yazyev, A. J. Austin, R. Cammi, C. Pomelli, J. W. Ochterski, R. L. Martin, K. Morokuma, V. G. Zakrzewski, G. A. Voth, P. Salvador, J. J. Dannenberg, S. Dapprich, A. D. Daniels, O. Farkas, J. B. Foresman, J. V. Ortiz, J. Cioslowski, D. J. Fox, Gaussian 09, Revision B.01; Gaussian, Inc., Wallingford CT, **2009**.
[34] T. Lavy, N. Meirovich, H. A. Sparkes, J. A. K. Howard, M. Kaftory, *Acta Cryst. C.* **2007**, *C63*, o89-o92
[35] R. Kar, S. Pal, *Int. J. Quantum Chem.* **2010**, *110*, 1642–1647.
[36] J–C. Fan, Z–C. Shang, J. Liang, X–H. Liu, H. Jin, *J. Mol. Struct.–Theochem.* **2010**, *939*, 106–111.
[37] K. B. Wiberg, D. J. Rush, *J. Am. Chem. Soc.* **2001**, *123*, 2038–2046.
[38] A. Liu, D. Wu, D. Jia, L. Liu, *Int. J. Quantum Chem.* **2010**, *110*, 1360–1367.
[39] D. K. Singh, S. K. Srivastava, A. K. Ojha, B. P. Asthana, *J. Mol. Struc.* **2008**, *892*, 384–391.
[40] J. P. Merrick, D. Moran, L. Radom, *J. Phys. Chem.* A **2007**, *111*, 11683–11700.
[41] D. Michalska, D. C. Bieńko, A. J. Abkowicz-Bieńko, Z. Latajka, *J. Phys. Chem.* 1996, 100, 17786–17790.
[42] K. Fukui, *Science* **1982**, *218*, 747–754.
[43] S. Gunasekaran, R. A. Balaji, S. Kumeresan, G. Anand, S. Srinivasan, *Can. J. Anal. Sci. Spectrosc.* **2008**, *53*, 149–162.
[44] K. Fukui, T. Yonezawa, H. Shingu, *J. Chem. Phys.* **1952**, *20*, 722–725.
[45] C. H. Choi, M. Kertesz, *J. Phys. Chem. A.* **1997**, *101*, 3823–3831.
[46] S. Iyasamy, K. Varadharajan, S. Sivagnanam, *Z. Phys. Chem.* **2016**, *230*, 1681–1710.
[47] T. S. Xavier, I. H. Joe, *Spectrochim. Acta A* **2011**, *79*, 332–337.

Submitted: February 12, 2018
Accepted: May 24, 2018

© 2018 Wiley-VCH Verlag GmbH & Co. KGaA, Weinheim